

**A nanocomposite optosensor containing carboxylic functionalized multiwall carbon nanotubes and quantum dots incorporated into a molecularly imprinted polymer for highly selective and sensitive detection of ciprofloxacin**

NaphatYuphintharakun<sup>1,2</sup>, Piyaluk Nurerk<sup>1,2</sup>, Kochaporn Chullasat<sup>1,2</sup>, Proespichaya Kanatharana<sup>1,2</sup>, Frank Davis<sup>3</sup>, Dhassida Sooksawat<sup>1,2</sup> and Opas Bunkoed<sup>1,2\*</sup>

<sup>1</sup>Trace Analysis and Biosensor Research Center, Prince of Songkla University, Hat Yai, Songkhla 90112, Thailand

<sup>2</sup>Center of Excellence for Innovation in Chemistry, Department of Chemistry, Faculty of Science, Prince of Songkla University, Hat Yai, Songkhla 90112, Thailand

<sup>3</sup>University of Chichester, College Lane, Chichester, West Sussex, P019 6PE, UK

**Corresponding author:** Tel: +66 74288443; Fax: +66 74558841

**Email address:** opas.b@psu.ac.th, opas1bunkoed@hotmail.com

### Abstract

A nanocomposite optosensor consisting of carboxylic acid functionalized multiwall carbon nanotubes and CdTe quantum dots embedded inside a molecularly imprinted polymer (COOH@MWCNT-MIP-QDs) was developed for trace ciprofloxacin detection. The COOH@MWCNT-MIP-QDs were synthesized through a facile sol-gel process using ciprofloxacin as a template molecule, 3-aminopropylethoxysilane as a functional monomer and tetraethoxysilane as a cross-linker at a molar ratio of 1:8:20. The synthesized nanocomposite optosensor had high sensitivity, excellent specificity and high binding affinity to ciprofloxacin. Under optimal conditions, the fluorescence intensity of the optosensor decreased in a linear fashion with the concentration of ciprofloxacin and two linear dynamic ranges were obtained, 0.10–1.0  $\mu\text{g L}^{-1}$  and 1.0–100.0  $\mu\text{g L}^{-1}$  with a very low limit of detection of 0.066  $\mu\text{g L}^{-1}$ . The imprinting factors of the two linear range were 17.67 and 4.28, respectively. The developed nanocomposite fluorescence probe was applied towards the determination of ciprofloxacin levels in chicken muscle and milk samples with satisfactory recoveries being obtained in the range of 82.6 to 98.4%. The results were also in good agreement with a HPLC method which indicates that the optosensor can be used as a sensitive, selective and rapid method to detect ciprofloxacin in chicken and milk sample.

**Keywords:** quantum dots, optosensor, multiwall carbon nanotube, molecularly imprinted polymer, ciprofloxacin

## 1. Introduction

Ciprofloxacin is a fluoroquinolone antibiotic which is widely used for the treatment of respiratory and digestive infections in humans and livestock [1]. This drug is also misused in the livestock industry since treating animals with these agents can increase productivity. However, this can become a serious problem, since the antibiotics can be expressed in meat and milk leading to potential toxicity [2] or allergic hypersensitivity reactions in humans. There is also a further serious issue that this practice may lead to the generation of antibiotic resistant human pathogens. Therefore, the European Union has set the maximum residue limit (MRL) for ciprofloxacin at  $100 \mu\text{g kg}^{-1}$  in milk, chicken and pig muscle [3]. Thus, it is necessary to develop a convenient, rapid and cost-effective method for the monitoring of ciprofloxacin in food samples. Several analytical techniques have been reported for ciprofloxacin detection such as high performance liquid chromatography [4-6], capillary electrophoresis [7] and electrochemical techniques [8-11]. However, these techniques can be complicated, may require expensive instrumentation and highly skilled personnel. To overcome these drawbacks, spectrofluorimetry can be considered as an alternative method due to its simplicity, rapidity and cost effectiveness. The sensitivity of this method can be improved using high sensitive fluorescence probes such as quantum dot nanoparticles (QDs). QDs have been used for the determination of various target analytes at trace levels typical analytes include salicylic acid [12], glucose [13],  $\text{H}_2\text{O}_2$  [14], 6-mercaptopurine [15], ochratoxin A [16], kaempferol [17] and copper (II) ion [18]. In addition, QDs have many unique optical properties such as tunable size-dependent photoluminescence, good photostability and narrow symmetric emissions [19, 20]. The determination of trace target analytes in real samples with high matrix interferences normally requires highly selective methods. To further improve the selectivity of these methods, molecularly imprinted polymers (MIPs) have received considerable study due to their high specificity and facile

preparation. MIPS are normally prepared by a co-polymerization process of cross-linker moieties with functional monomers that form complexes with analytes (template molecule) prior to polymerization. After the template molecules were eluted from the polymer, specific recognition sites which are complementary in size, shape and functional groups to the template can be obtained, leading to the ability to rebind template molecules with high specificity. MIPS not only provide highly selective binding material but also have high stability meaning they can be used under extreme condition such as extreme pH, high temperature and in organic solvents. Since MIPS are cost-effective and robust materials, they have been extensively used in many fields such as an adsorbent material [21], solid phase microextraction [22-24] and chemosensors and biosensors [25-27]. For sensor applications, the composite fluorescence probes using QDs incorporated into MIPS have been developed as highly selective fluorescence probes for the determination of some target compounds such as salbutamol [28], patulin [29], sulfadiazine [30], sulfadimidine [31], malachite green [32], tetracycline [33], cocaine [34] and amoxicillin [35]. To improve the kinetic adsorption or affinity binding of ciprofloxacin, addition of carboxylic acid functionalized multiwall carbon nanotubes is an interesting alternative approach since they contain an extended  $\pi$  structure which can adsorb aromatic compounds via  $\pi$ - $\pi$  interactions [36]. The carboxylic acid functionalisation of multiwall carbon nanotubes can improve their dispersibility in aqueous media and it is easy to achieve further covalent functionalisation with other materials [37].

In this work, nanocomposite optosensor COOH functionalized MWCNTs and CdTe quantum dots embedded in a MIPS were synthesized for trace ciprofloxacin detection. The determination of ciprofloxacin is based on the fluorescence quenching when target analyte is bound to the binding sites on the developed fluorescence probes. This integrated the desirable optical properties of the quantum dots with the high specificity of MIPS and high adsorption affinity of COOH@MWCNT to produce a rapid, highly sensitive optosensor for the

determination of ciprofloxacin with good selectivity. The developed optosensor was applied to determine ciprofloxacin in chicken muscle and milk and the accuracy of the method was investigated by comparing with a HPLC technique.

## **2. Experimental**

### **2.1 Chemicals and reagents**

Tellurium powder (99.8%), sodium borohydride ( $\text{NaBH}_4$ ), thioglycolic acid (TGA), 3-aminopropyltriethoxysilane (APTES), cadmium chloride ( $\text{CdCl}_2 \cdot \text{H}_2\text{O}$ ) and tetraethylorthosilicate (TEOS) were from Sigma-Aldrich (St. Louis, MO, USA). Ciprofloxacin was supplied by Tokyo Chemical Industry (Tokyo, Japan), Tris (hydroxymethyl) aminomethane and methanol were obtained from Merck (Darmstadt, Germany), 25%  $\text{NH}_3 \cdot \text{H}_2\text{O}$  was from QReC (New Zealand). MWCNTs were purchased from Shenzhen Nano-Technologies Port Co., Ltd. (China), Rhodamine 6G was purchased from Tokyo Chemical Industry (Tokyo, Japan). Deionised water (18.2  $\text{M}\Omega \text{ cm}$ ) was produced by an Elgastat Maxima water system (ELGA, High Wycombe, UK).

### **2.2 Apparatus**

Fluorescence spectra were recorded using a RF-5301 spectrofluorometer (Shimadzu, Tokyo, Japan). An Avaspec 2048 spectrometer (Apeldoorn, The Netherlands) was used to record ultraviolet-visible absorption spectra and Fourier transform infrared (FT-IR) spectra were obtained using a Spectrum BX FTIR spectroscope (PerkinElmer, Waltham, MA, USA) on solid samples dispersed within KBr discs. Scanning electron microscope (SEM) images were obtained using a JSM-5200 microscope (JEOL, Tokyo, Japan). Transmission electron micrograph (TEM) images were obtained using a JEM-2010 microscope (JEOL, Tokyo, Japan). The surface areas were measured with an ASAP 2460 surface area and porosity analyzer (Micromeritics, Norcross, USA).

### **2.3 Synthesis of thioglycolic acid-capped CdTe quantum dots**

The synthesis of TGA-capped CdTe QDs were performed as previously reported with some modification [38]. Briefly, 0.050 g of Te powder and 0.045 g of NaBH<sub>4</sub> were dissolved in 2.0 mL of deionised water to prepare a NaHTe solution. Separately, 0.046 g of CdCl<sub>2</sub>·H<sub>2</sub>O and 30 μL of TGA were mixed with 100 mL of deionised water and adjusted to pH 11.50 using 1.0M NaOH. The solution was heated under nitrogen atmosphere until the temperature was 90°C and then 0.50 mL of the NaHTe aqueous solution was injected into the solution and the mixture refluxed for 10min. The TGA-capped CdTe QDs were precipitated with ethanol and centrifuged at 6000 rpm for 15 min to eliminate the excess reagents. The TGA-capped CdTe QDs were dried in an oven at 50°C for 4 h and kept in a desiccator at room temperature (25 °C) until used.

#### **2.4 Synthesis of nanocomposite COOH@MWCNT-MIP-QDs fluorescence probe**

The carboxylic functionalized multiwall carbon nanotubes and QDs were incorporated into MIP via a sol-gel copolymerization process. Briefly, 8.3 mg of ciprofloxacin (template) was dissolved in 10 mL of deionised water and 0.0050 g of COOH@MWCNT was added to the solution. Then, 48.0 μL of APTES and 5.0 mL of CdTe QDs were sequentially added in the mixture solution and stirred for 1 h. Subsequently, 110μL of TEOS and 150 μL of ammonia solution (25 wt %) were added to the solution and continuously stirred for 5 h. After polymerization, the nanocomposite COOH@MWCNT-MIP-QDs were obtained and the template removed by washing with three portions of 10 mL of ethanol, the process of template removal was investigated by measuring the washing solutions absorption at 260 nm. The nanocomposite COOH@MWCNTs-MIP-QDs were collected by centrifugation at 5000 rpm for 15 min and dried at 50°C for 4 h. The nanocomposite non-imprinted polymer (COOH@MWCNTs-NIP-QDs) was also prepared using identical conditions except without the addition of template (ciprofloxacin).

#### **2.5 Fluorescence measurement**

The nanocomposite COOH@MWCNT-MIP-QDs were dispersed in 0.010 M Tris-HCl buffer solution (pH 7.0) and 150  $\mu\text{L}$  was mixed with 50  $\mu\text{L}$  of ciprofloxacin standard solution under rotation for 15 min. The mixture was transferred into a quartz cell and its fluorescence intensity measured by setting the excitation wavelength at 272 nm and recording in the emission range of 400–700 nm. The slit widths of the excitation and emission were both 10 nm. The measurement was performed at room temperature (25  $^{\circ}\text{C}$ ) for convenience of analysis.

## **2.6 Sample preparation**

The chicken muscle and milk samples were collected from local markets in Hat Yai city, Thailand. Extraction of ciprofloxacin from chicken muscle was carried out as described in a previous report [39]. Briefly, 300  $\mu\text{L}$  of Tris buffer solution (pH 7.0) was added to 0.50 g of homogenized chicken muscle and vortexed for 1 min. Acetonitrile (1.0 mL) was added into the mixture which was vortexed for another 1 min and then sonicated for 10 min. The supernatant was separated and mixed with 300  $\mu\text{L}$  of hexane into a 15 mL centrifuge tube and vortexed for 1 min. The extract was centrifuged at 6000 rpm to remove the degreasing phase. The acetonitrile phase was then evaporated to dryness at 50  $^{\circ}\text{C}$  and redissolved with 10 mL deionised water and filtered through a 0.22  $\mu\text{m}$  syringe filter before analysis with the developed method.

The extraction procedure of ciprofloxacin from milk was adapted from previous work [40]. Briefly, 10.0 mL of the milk sample and 10 mL of acetonitrile were added into a 50 mL centrifuge tube followed by vortexing for 5 min and centrifuged at 6000 rpm for 30 min. Then, the supernatant was separated and evaporated to dryness at 50 $^{\circ}\text{C}$ , the dried extract was redissolved in 10.0 mL deionised water before mixing with the developed fluorescence probe for analysis.

## **2.7 Analysis by HPLC method**

HPLC analyses were carried out using an Agilent 1100 series HPLC system (Germany). The analytical column was a VertiSep<sup>TM</sup> UPS C18 column (4.6×150mm, 5μm). Acetonitrile (18%) and 25mM H<sub>3</sub>PO<sub>4</sub> (82%) was used as the mobile phase at a flow rate of 0.9 mL min<sup>-1</sup>. The sample volume was 20 μL. The excitation ( $\lambda_{ex}$ ) and emission ( $\lambda_{em}$ ) wavelength were 272 and 448 nm, respectively.

### 3. Results and discussion

#### 3.1 The synthesis of nanocomposite COOH@MWCNT-MIP-QDs optosensors for ciprofloxacin detection

The nanocomposite COOH@MWCNT-MIP-QDs optosensor were prepared via copolymerization process incorporating COOH@MWCNT, TGA-capped CdTe QDs, APTES (functional monomer), TEOS (cross-linker), ciprofloxacin (template) and NH<sub>3</sub>(catalyst). The carboxylic groups of TGA-capped CdTe QDs and COOH@MWCNT can interact with amino groups (-NH<sub>2</sub>) of APTES to facilitate incorporation of the CdTe QDs into the sol-gel via hydrogen bonding. Also, non-covalent interaction between APTES and ciprofloxacin (template) occurred during the molecularly imprinting process, for example the amino group can interact with the carboxylic group of ciprofloxacin through hydrogen bonding. COOH@MWCNT can interact with ciprofloxacin via  $\pi$ - $\pi$  interaction and also hydrogen bonding (**Fig.1**).

The synthesized nanocomposite COOH@MWCNT-MIP-QDs optosensors showed a highly symmetric emission at 544 nm. **Fig. 2** displays the fluorescence spectra of COOH@MWCNT-NIP-QDs (spectrum a), COOH@MWCNT-MIP-QDs after washing during which the template was removed (spectrum b) and COOH@MWCNT-MIP-QDs prior to removal of template molecules (spectrum c). Before template removal the fluorescence intensity of COOH@MWCNT-MIP-QDs was relatively low, about 50% of that of the NIP, while after removal of template molecule its fluorescence intensity was restored to almost the

same level as found for NIP-QDs (97.0%). This result confirms that the ciprofloxacin (template) was completely removed from the MIP layer. This facile synthesis method can be performed under mild conditions at room temperature (27 °C).

### 3.2 Characterization of nanocomposite COOH@MWCNT-MIP-QDs optosensor

Fluorescence and UV-Vis spectrum of CdTe QDs are shown in **Fig. S1**. TGA-capped CdTe QDs showed a narrow and symmetric fluorescence spectrum with the maximum emission wavelength being 540nm. The calculated particle size of the TGA-capped CdTe QDs was 2.10nm using the method described in previous work [12].

**Fig. 3A** and **3B** shows the TEM images of TGA-capped CdTe QDs and nanocomposite MIP-QDs. The QDs nanoparticles were distributed within the MIP layer of the nanocomposite fluorescence probe. The results of TEM imaging confirm that QDs were embedded into the molecularly imprinted polymer matrix. The morphological structures of nanocomposite COOH@MWCNT-MIP-QDs were also investigated by the SEM technique (**Fig. 3C**). They exhibit a rough surface which indicated that specific recognition sites presented in the nanocomposite fluorescence probe.

FT-IR spectroscopy was performed to investigate the functional groups of the nanocomposite optosensor. **Fig. 4a** shows the characteristic peaks of TGA-capped CdTe QDs, the absorption peaks at 1375 and 1582  $\text{cm}^{-1}$  are due to the symmetric and asymmetric stretching of the carboxylate group. Bands at 1224 and 3448  $\text{cm}^{-1}$  are the stretching vibration of C-O and O-H, respectively. FT-IR spectrum of ciprofloxacin (**Fig. 4b**) showed characteristic peaks at 1050  $\text{cm}^{-1}$  due to C-F stretching and peaks at 1410  $\text{cm}^{-1}$  and 1620  $\text{cm}^{-1}$  due to C=O stretching and N-H bending of the quinolone ring [41], respectively. The absorption peak at 2900  $\text{cm}^{-1}$  was due to C-H stretching. **Fig. 4c** shows the FT-IR spectrum of hybrid nanocomposite COOH@MWCNT-MIP-QDs optosensor before removal of template (ciprofloxacin). The characteristic peak at 1060  $\text{cm}^{-1}$  corresponded to Si-O-Si asymmetric

stretching. Absorption peaks at around 460 and 760  $\text{cm}^{-1}$  are assigned to the Si-O vibration band and the broad absorption band at 3440  $\text{cm}^{-1}$  corresponds to N-H stretching of aminopropyl group. After removal of template the characteristic peaks which related to ciprofloxacin disappear (**Fig. 4d**). The band around 1628  $\text{cm}^{-1}$  was due to the C=C stretching of the carbon nanotube backbones (**Fig. 4e**). These results indicated that a hybrid nanocomposite COOH@MWCNT-MIP-QDs was successfully synthesized for selective recognition for ciprofloxacin.

The fluorescence quantum yield of CdTe QDs, MIP-QDs and COOH@MWCNT-MIP-QDs were 0.89 and 0.62 and 0.48 respectively, using Rhodamine 6G as a reference [42]. The BET surface areas of COOH@MWCNT-NIP-QDs and COOH@MWCNT-MIP-QDs were 15.75 and 23.46  $\text{m}^2\text{g}^{-1}$  respectively. The nanocomposite COOH@MWCNT-MIP-QDs optosensor showed higher surface area than NIP-QDs, possibly because of the imprinted sites of the template.

### 3.3 Optimization of the analysis system

Several parameters influencing the fluorescence quenching of nanocomposite COOH@MWCNT-MIP-QDs optosensors for ciprofloxacin detection *i.e.* incubation time, pH, amount of COOH@MWCNT as well as the ratios of template to cross-linker and template to monomer were optimized. The highest quenching efficiency (sensitivity) and the shortest analysis time were considered to be the optimum values.

#### 3.3.1 Effect of the adsorption time

To investigate the binding performances of nanocomposite COOH@MWCNT-MIP-QDs and MIP-QDs with ciprofloxacin, the effects of adsorption time were investigated. The fluorescence intensity of COOH@MWCNT-MIP-QDs and MIP-QDs showed significant increases up to adsorption times of 15 min and 22 min, respectively (**Fig. S2**). With longer exposures, the fluorescence intensity remained almost constant with further increases in

adsorption time. The equilibrium binding of COOH@MWCNT-MIP-QDs was faster than MIP-QDs by about 7 min which indicated that COOH@MWCNT can help to improve mass-transfer speed between the ciprofloxacin and its recognition sites. Thus, nanocomposite COOH@MWCNT-MIP-QDs was used as a rapid fluorescence probe for ciprofloxacin detection.

### 3.3.2 Effect of pH

The pH level had significant effects on fluorescence quenching of QDs due to their sensitivity to the surrounding environment such as acids, bases, metal ions and organic molecules [18, 43]. In this work, the effect of pH between 6.0 to 9.0 on the determination of ciprofloxacin was investigated. The results are shown in **Fig. 5A**; with highest fluorescence quenching being obtained at a pH of 7.0. Since, the template molecules and MIPs are bound through hydrogen bonding, the binding efficiency was decreased by hydrogen ion under acidic medium ( $\text{pH} < 7$ ) which causes a decrease in the interaction between template molecule and binding site. The fluorescence quenching was also decreased at pH higher than 7.0 due to the degradation or ionization of the template molecule under alkaline conditions. Moreover, the silica layer was unstable and will ionize in an alkaline solution which can cause damage to the binding site of nanocomposite COOH@MWCNT-MIP-QDs probe thereby affecting the interaction between template and optosensing probe [44]. Therefore, a Tris-HCl buffer solution (pH 7.0) was chosen as an optimum binding media and used for further experiments.

### 3.3.3 Amount of carboxylic functionalized multiwall carbon nanotubes (COOH@MWCNTs)

The effect of the amount of COOH@MWCNT in nanocomposite fluorescence probe was also optimized to obtain the high sensitivity for the determination of ciprofloxacin. The highest sensitivity was obtained using an amount of COOH@MWCNT of 0.0005% w/v (**Fig. 5B**). At lower levels of COOH@MWCNT, the composites showed lower sensitivity, possibly

the adsorption was not complete with an incubation time of 15 min. However, the sensitivity was also decreased at higher levels of COOH@MWCNT; this could be possibly due to the MWCNTs disrupting the polymer structure, leading to the decrease of the number of recognition sites in the MIP layer. Therefore, 0.0005 % w/v of COOH@MWCNT was selected for further experiment.

### 3.3.4 Ratio of template to cross-linker

TEOS is normally used as cross-linker to prepare MIPs and it can affect the recognition ability of the MIPs [31, 45]. Thus, the effect of molar ratio of template to cross-linker was investigated to obtain the highest sensitivity for the determination of ciprofloxacin. As shown in **Fig. 5C**, a 1:20 template to cross-linker molar ratio provided the highest sensitivity. The sensitivity was decreased at lower amount of cross-linker (1:10) due to lower levels of crosslinking leading to the MIP-QDs structure being physically weaker and allowing an increase of molecular movement causing the formation of recognition sites to be less effective. The sensitivity was also decreased at higher amount of cross-linker (1:30 and 1:40) because a large amount of cross-linker results in a highly rigid polymer, providing highly rigid recognition sites. Also, excessive cross-linking can block the movement of functional monomer which reduces the target analyte and functional monomer interaction [46]. Therefore, a molar ratio of ciprofloxacin to TEOS of 1:20 was chosen for further experiment.

### 3.3.5 Ratio of template to monomer

The nanocomposite COOH@MWCNT-MIP-QDs fluorescence probe was synthesized using APTES as functional monomer and it is an important factors on the specific recognition sites of MIP layer [47]. In this work, the molar ratio of template to monomer was investigated with the highest sensitivity being obtained for a 1:8 template to functional monomer (APTES) molar ratio (**Fig. 5D**). The lower amount of functional monomer (1:4 and 1:6) would produce a low number of recognition site ( $-NH_2$  group) to interact with target analyte via hydrogen

bonding. Also, the sensitivity was decreased at a higher amount of functional monomer (1:10) due to the excess functional monomer forming non-imprinted layers within the polymer which might inhibit the binding between target analyte and recognition sites. Thus, the molar ratio of ciprofloxacin to APTES of 1:8 was selected for subsequent experiment.

### **3.4 Comparison of different fluorescence probes**

The sensitivity of different fluorescence probes were investigated for the determination of ciprofloxacin including NIP-QDs, COOH@MWCNT-NIP-QDs, MIP-QDs and COOH@MWCNT-MIP-QDs. As shown in **Fig. 6**. NIP-QDs showed the lowest sensitivity for ciprofloxacin detection due to the fact that they have no specific imprinted cavities for ciprofloxacin, the functional monomers were randomly orientated in the particles leading to low adsorption ability. The sensitivity was increased on incorporation of COOH@MWCNT in NIP-QDs, this is because ciprofloxacin could adsorb on the surface of COOH@MWCNT via  $\pi$ - $\pi$  interactions leading to an increase in the quenching efficiency for ciprofloxacin detection. The nanocomposite MIP-QDs showed higher sensitivity than both NIP-QDs and COOH@MWCNT-NIP-QDs due to many specific binding sites being present in the fluorescence probes which can selectively interact with template molecule. The highest sensitivity was obtained for a nanocomposite COOH@MWCNT-MIP-QDs due to the integration of high affinity of COOH@MWCNT with ciprofloxacin and specific recognition cavities of MIP. These results confirm that the combination of COOH@MWCNT, MIP and QDs could improve the sensitivity, specificity and adsorption speed.

### **3.5 Fluorescence quenching mechanism**

The fluorescence quenching mechanism of nanocomposite COOH@MWCNT-MIP-QDs by ciprofloxacin was described. Hydrogen bonding could occur between ciprofloxacin and the  $\text{NH}_2$  groups of functional monomer on the surface of fluorescence probe. This led to the possibility that the electrons of the QDs conduction bands could be transferred into the

lowest unoccupied molecular orbital of ciprofloxacin leading to the fluorescence quenching [48]. Thus, the fluorescence quenching of nanocomposite COOH@MWCNT-MIP-QDs is due to an electron transfer mechanism from QDs to ciprofloxacin. In addition, energy transfer was not considered to be a possible mechanism due to there being no spectral overlap between the COOH@MWCNT-MIP-QDs emission spectrum and the ciprofloxacin absorption spectrum [33, 42] (**Fig. S3**).

The fluorescence quenching of the system was described using the Stern-Volmer equation:

$$F_0/F = 1 + K_{sv}[C]$$

Where  $F$  and  $F_0$  are the fluorescence intensity of nanocomposite COOH@MWCNT-MIP-QDs fluorescence probe in the presence and absence of quencher (ciprofloxacin), respectively.  $K_{sv}$  the quenching constant and  $[C]$  the quencher concentration. The imprinting factor (IF) was calculated from the ratio of  $K_{SV,MIP}$  to  $K_{SV,NIP}$ .

### **3.6 Selectivity of nanocomposite COOH@MWCNT-MIP-QDs for the determination of ciprofloxacin**

The fluorescence quenching of nanocomposite COOH@MWCNT-MIP-QDs towards other ciprofloxacin structural analogs (danofloxacin, difloxacin, enrofloxacin, norfloxacin, sarafloxacin) were investigated to study its selectivity since hydrogen bonds can form between the structural analogs and the functional groups located in the imprinting sites. As shown in **Fig. 7**, the nanocomposite COOH@MWCNT-MIP-QDs had higher fluorescence quenching than other nanocomposites. This is because during the synthesis process of nanocomposite COOH@MWCNT-MIP-QDs, many specific imprinting sites which act as a memory of the shape, size and functional groups of ciprofloxacin were generated. However, the nanocomposite COOH@MWCNT-NIP-QDs showed low fluorescence quenching to ciprofloxacin and other compounds due to no recognition sites existing in the NIP layer and

the molecules were adsorbed on the surface of NIP only through non-specific binding. A competitive binding experiment was also undertaken as shown in **Fig. 7** (inset). The sensitivities were not significantly changed by increasing of the ratio of  $C_{\text{Danofloxacin}}/C_{\text{Ciprofloxacin}}$  which indicated that the recognition sites are specific to the template molecule (ciprofloxacin).

### **3.7 Analytical performance of nanocomposite COOH@MWCNT-MIP-QDs for the determination of ciprofloxacin**

The analytical performances of the developed nanocomposite COOH@MWCNT-MIP-QDs optosensor were investigated including linearity, limit of detection (LOD) and limit of quantification (LOQ). As shown in **Fig. 8A**, two linear relationships of calibration curve were found with ranges of 0.10-1.0  $\mu\text{g L}^{-1}$ ;  $F_0/F = (0.159 \pm 0.008) + (1.038 \pm 0.005)$  (**Fig. 8B**) and 1.0-100.0  $\mu\text{g L}^{-1}$ ;  $F_0/F = (0.0060 \pm 0.0002) + (1.206 \pm 0.009)$  (**Fig. 8C**). The fact that two linear calibration curves were obtained might be due to the inhomogeneity of the specific imprinting cavities on the surface of the MIP. The imprinting factors were 17.67 and 4.28, respectively. The fluorescence spectra of nanocomposite COOH@MWCNT-MIP-QDs after mixing with various concentrations of ciprofloxacin were shown in **Fig. 8D**, the fluorescence intensities were significantly quenched by ciprofloxacin. The insets are the photographs of nanocomposite COOH@MWCNT-MIP-QDs in the presence (right) and absence (left) of ciprofloxacin under UV light. The LOD and LOQ calculated following the IUPAC criteria were 0.066  $\mu\text{g L}^{-1}$  and 0.22  $\mu\text{g L}^{-1}$ , respectively.

### **3.8 Reproducibility and stability of COOH@MWCNT-MIP-QDs**

The reproducibility of the nanocomposite COOH@MWCNT-MIP-QDs optosensors were investigated by preparing six different batches of nanocomposite COOH@MWCNT-MIP-QDs under the optimal conditions at different times. The developed optosensors were used to determine ciprofloxacin in the concentration range of 1.0-50.0  $\mu\text{g L}^{-1}$  and the

sensitivity was used to evaluate the reproducibility. The relative standard deviation (RSD) of sensitivities of the six optosensing systems was 1.5 %, indicating good batch-to-batch reproducibility.

The stability of nanocomposite COOH@MWCNT-MIP-QDs and CdTe QDs were also investigated by the repeated measurement of fluorescence intensity at room temperature (25 °C). The fluorescence intensity of nanocomposite COOH@MWCNT-MIP-QDs did not significantly change within 300 min, while the CdTe QDs fluorescence intensity was decreased after 90 min (**Fig. S4**). It could be deduced that the presence of a protective MIP layer helps to enhance the photostability of QDs.

### **3.9 Application of nanocomposite COOH@MWCNT-MIP-QDs optosensors for the determination of ciprofloxacin in food sample**

The developed nanocomposite COOH@MWCNT-MIP-QDs fluorescence probe was applied to determine ciprofloxacin in chicken muscle and milk (**Table 1**). Low concentrations of ciprofloxacin were found in chicken muscle ( $0.19 \mu\text{g kg}^{-1}$ ) and milk ( $0.22\text{-}0.35 \mu\text{g kg}^{-1}$ ) which were lower than the MRL value set by European Union ( $100 \mu\text{g kg}^{-1}$ ) for chicken muscle and milk. The accuracy of the developed optosensor was also investigated by spiking standard ciprofloxacin into real samples at different concentrations. Satisfactory recoveries between 82.6-98.4% were obtained with the relative standard deviation being lower than 8 %.

The spiked samples could also be extracted and analyzed using HPLC methods. **Fig. 9A** shows HPLC chromatograms of spiked samples at different concentration of ciprofloxacin. The correlation between the developed optosensors and HPLC was very good with the coefficient of determination being 0.9987 (**Fig. 9B**). The results indicated that the developed nanocomposite COOH@MWCNT-MIP-QDs fluorescence probes can be used as a simple, rapid and sensitive method to detect trace ciprofloxacin in milk and chicken muscle.

### **3.10 Comparison of the developed hybrid nanocomposite COOH@MWCNT-MIP-QDs optosensor with other methods**

The analytical performance of the developed optosensor for the determination of ciprofloxacin was compared to other works. As summarized in **Table 2**, the developed protocol provided a wide linear range and the detection limits are much lower than other work which demonstrates that the nanocomposite COOH@MWCNT-MIP-QDs are highly sensitive and selective for ciprofloxacin detection. The recovery (82.6-98.4%) and precision (<8%) of this method was comparable to other methods. This developed optosensor is simple, faster and lower cost than chromatographic techniques which require expensive instrumentation and potentially use large amounts of organic solvents as mobile phase. In addition, the selectivity of this sensor was improved with the use of MIPs, without requiring complicated separation processes crucial for many other methods.

### **4. Conclusion**

A nanocomposite COOH@MWCNT-MIP-QDs optosensor was developed for the determination of ciprofloxacin based on the electron transfer induced fluorescence quenching. The developed optosensor combined the high specificity of MIPs with the excellent optical properties of QDs with the high affinity of COOH@MWCNT to ciprofloxacin, thereby demonstrating a highly selective, sensitive and rapid method for the determination of trace ciprofloxacin. This rapid, convenient and cost-effective hybrid nanocomposite optosensor was successfully applied to determine ciprofloxacin in milk and chicken muscle with a satisfactory recovery and also demonstrated excellent agreement with HPLC. This facile and versatile process for optosensor fabrication provides potentially alternative methods for the specific recognition of many other organic compounds.

### **Acknowledgements**

This work was supported by the budget revenue of Prince of Songkla University (SCI600559S), the Thailand research fund, Center for Innovation in Chemistry (PERCH-CIC). Naphat Yuphintharakun was supported by the faculty of Science Research Fund, Prince of Songkla University, Hat Yai, Thailand, Contract no. 1-2559-02-009.

## References

- [1] P. Gayen, B.P. Chaplin, Selective Electrochemical detection of ciprofloxacin with a porous nafion/multiwalled carbon nanotube composite film electrode, *ACS Appl. Mater. Interfaces* 8 (2016) 1615-1626.
- [2] I.M. Velissariou, The use of fluoroquinolones in children: Recent advances, *Expert Rev Anti Infect Ther* 4 (2006) 853-860.
- [3] D. Gendrel, M. Chalumeau, F. Moulin, J. Raymond, Fluoroquinolones in paediatrics: a risk for the patient or for the community?, *Lancet Infect Dis* 3 (2003) 537-546.
- [4] M. Locatelli, M.T. Ciavarella, D. Paolino, C. Celia, E. Fiscarelli, G. Ricciotti, A. Pompilio, G. Di Bonaventura, R. Grande, G. Zengin, L. Di Marzio, Determination of ciprofloxacin and levofloxacin in human sputum collected from cystic fibrosis patients using microextraction by packed sorbent-high performance liquid chromatography photodiode array detector, *J Chromatogr A* 1419 (2015) 58-66.
- [5] J. Vella, F. Busuttil, N.S. Bartolo, C. Sammut, V. Ferrito, A. Serracino-Inglott, L.M. Azzopardi, G. LaFerla, A simple HPLC-UV method for the determination of ciprofloxacin in human plasma, *J Chromatogr B* 989 (2015) 80-85.
- [6] B. Chen, J. Han, Y. Wang, C. Sheng, Y. Liu, G. Zhang, Y. Yan, Separation, enrichment and determination of ciprofloxacin using thermoseparating polymer aqueous two-phase system combined with high performance liquid chromatography in milk, egg, and shrimp samples, *Food Chem.* 148 (2014) 105-111.

- [7] D. Moreno-González, A.M. Hamed, B. Gilbert-López, L. Gámiz-Gracia, A.M. García-Campaña, Evaluation of a multiresidue capillary electrophoresis-quadrupole-time-of-flight mass spectrometry method for the determination of antibiotics in milk samples, *J Chromatogr A* 1510 (2017) 100-107.
- [8] J. Shan, R. Li, K. Yan, Y. Zhu, J. Zhang, In situ anodic stripping of Cd(II) from CdS quantum dots for electrochemical sensing of ciprofloxacin, *Sens. Actuators B* 237 (2016) 75-80.
- [9] H. Bagheri, H. Khoshsafar, S. Amidi, Y. Hosseinzadeh Ardakani, Fabrication of an electrochemical sensor based on magnetic multi-walled carbon nanotubes for the determination of ciprofloxacin, *Anal. Methods* 8 (2016) 3383-3390.
- [10] G. Tsekenis, G.Z. Garifallou, F. Davis, P.A. Millner, D.G. Pinacho, F. Sanchez-Baeza, M.P. Marco, T.D. Gibson, S.P.J. Higson, Detection of fluoroquinolone antibiotics in milk via a labelless immunoassay based upon an alternating current impedance protocol, *Anal. Chem.* 80 (2008) 9233-9239.
- [11] G.Z. Garifallou, G. Tsekenis, F. Davis, S.P.J. Higson, P.A. Millner, D.G. Pinacho, F. Sanchez-Baeza, M.P. Marco, T.D. Gibson, Labelless immunosensor assay for fluoroquinolone antibiotics based upon an AC impedance protocol, *Anal Lett* 40 (2007) 1412-1422.
- [12] O. Bunkoed, P. Kanatharana, Mercaptopropionic acid-capped CdTe quantum dots as fluorescence probe for the determination of salicylic acid in pharmaceutical products, *Luminescence* 30 (2015) 1083-1089.
- [13] M. Yu, K. Zhao, X. Zhu, S. Tang, Z. Nie, Y. Huang, P. Zhao, S. Yao, Development of near-infrared ratiometric fluorescent probe based on cationic conjugated polymer and CdTe/CdS QDs for label-free determination of glucose in human body fluids, *Biosens. Bioelectron.* 95 (2017) 41-47.

- [14] T. Gong, J. Liu, Y. Wu, Y. Xiao, X. Wang, S. Yuan, Fluorescence enhancement of CdTe quantum dots by HBcAb-HRP for sensitive detection of H<sub>2</sub>O<sub>2</sub> in human serum, *Biosens. Bioelectron.* 92 (2017) 16-20.
- [15] M. Jin, Z.L. Mou, R.L. Zhang, S.S. Liang, Z.Q. Zhang, An efficient ratiometric fluorescence sensor based on metal-organic frameworks and quantum dots for highly selective detection of 6-mercaptopurine, *Biosens. Bioelectron.* 91 (2017) 162-168.
- [16] J. Yao, G. Xing, J. Han, Y. Sun, F. Wang, R. Deng, X. Hu, G. Zhang, Novel fluoroimmunoassays for detecting ochratoxin A using CdTe quantum dots, *J. Biophotonics* 10 (2017) 657-663.
- [17] X. Tan, S. Liu, Y. Shen, Y. He, J. Yang, Quantum dots (QDs) based fluorescence probe for the sensitive determination of kaempferol, *Spectrochim. Acta A* 133 (2014) 66-72.
- [18] S. Geng, S.M. Lin, N.B. Li, H.Q. Luo, Polyethylene glycol capped ZnO quantum dots as a fluorescent probe for determining copper(II) ion, *Sens. Actuators B* 253 (2017) 137-143.
- [19] R.M. Amin, S.A. Elfeky, T. Verwanger, B. Krammer, Fluorescence-based CdTe nanosensor for sensitive detection of cytochrome C, *Biosens. Bioelectron.* 98 (2017) 415-420.
- [20] J. Zhu, Z.J. Zhao, J.J. Li, J.W. Zhao, Fluorescent detection of ascorbic acid based on the emission wavelength shift of CdTe quantum dots, *J. Lumin.* 192 (2017) 47-55.
- [21] G. Theodoridis, M. Lasáková, V. Škeříková, A. Tegou, N. Giantsiou, P. Jandera, Molecular imprinting of natural flavonoid antioxidants: Application in solid-phase extraction for the sample pretreatment of natural products prior to HPLC analysis, *J. Sep. Sci.* 29 (2006) 2310-2321.
- [22] H. Asiabi, Y. Yamini, S. Seidi, F. Ghahramanifard, Preparation and evaluation of a novel molecularly imprinted polymer coating for selective extraction of indomethacin from

biological samples by electrochemically controlled in-tube solid phase microextraction, *Anal. Chim. Acta* 913 (2016) 76-85.

[23] Z. Terzopoulou, M. Papageorgiou, G.Z. Kyzas, D.N. Bikiaris, D.A. Lambropoulou, Preparation of molecularly imprinted solid-phase microextraction fiber for the selective removal and extraction of the antiviral drug abacavir in environmental and biological matrices, *Anal. Chim. Acta* 913 (2016) 63-75.

[24] T. Zhao, X. Guan, W. Tang, Y. Ma, H. Zhang, Preparation of temperature sensitive molecularly imprinted polymer for solid-phase microextraction coatings on stainless steel fiber to measure ofloxacin, *Anal. Chim. Acta* 853 (2015) 668-675.

[25] J. Ji, Z. Zhou, X. Zhao, J. Sun, X. Sun, Electrochemical sensor based on molecularly imprinted film at Au nanoparticles-carbon nanotubes modified electrode for determination of cholesterol, *Biosens. Bioelectron.* 66 (2015) 590-595.

[26] A. Kumar Singh, M. Singh, QCM sensing of melphalan via electropolymerized molecularly imprinted polythiophene films, *Biosens. Bioelectron.* 74 (2015) 711-717.

[27] X. Zhou, X. Gao, F. Song, C. Wang, F. Chu, S. Wu, A sensing approach for dopamine determination by boronic acid-functionalized molecularly imprinted graphene quantum dots composite, *Appl. Surf. Sci.* 423 (2017) 810-816.

[28] P. Raksawong, K. Chullasat, P. Nurerk, P. Kanatharana, F. Davis, O. Bunkoed, A hybrid molecularly imprinted polymer coated quantum dot nanocomposite optosensor for highly sensitive and selective determination of salbutamol in animal feeds and meat samples, *Anal. Bioanal. Chem.* 409 (2017) 4697-4707.

[29] W. Zhang, Y. Han, X. Chen, X. Luo, J. Wang, T. Yue, Z. Li, Surface molecularly imprinted polymer capped Mn-doped ZnS quantum dots as a phosphorescent nanosensor for detecting patulin in apple juice, *Food Chem.* 232 (2017) 145-154.

- [30] H. Ding, H.F. Jiao, X.Z. Shi, A.L. Sun, X.Q. Guo, D.X. Li, J. Chen, Molecularly imprinted optosensing sensor for highly selective and sensitive recognition of sulfadiazine in seawater and shrimp samples, *Sens. Actuators B* 246 (2017) 510-517.
- [31] Z. Zhou, H. Ying, Y. Liu, W. Xu, Y. Yang, Y. Luan, Y. Lu, T. Liu, S. Yu, W. Yang, Synthesis of surface molecular imprinting polymer on SiO<sub>2</sub>-coated CdTe quantum dots as sensor for selective detection of sulfadimidine, *Appl. Surf. Sci.* 404 (2017) 188-196.
- [32] L. Wu, Z.Z. Lin, H.P. Zhong, X.M. Chen, Z.Y. Huang, Rapid determination of malachite green in water and fish using a fluorescent probe based on CdTe quantum dots coated with molecularly imprinted polymer, *Sens. Actuators B* 239 (2017) 69-75.
- [33] L. Zhang, L. Chen, Fluorescence Probe Based on Hybrid Mesoporous Silica/Quantum Dot/Molecularly Imprinted Polymer for Detection of Tetracycline, *ACS Appl. Mater. Interfaces* 8 (2016) 16248-16256.
- [34] M.P. Chantada-Vázquez, J. Sánchez-González, E. Peña-Vázquez, M.J. Taberero, A.M. Bermejo, P. Bermejo-Barrera, A. Moreda-Piñeiro, Simple and Sensitive Molecularly Imprinted Polymer - Mn-Doped ZnS Quantum Dots Based Fluorescence Probe for Cocaine and Metabolites Determination in Urine, *Anal. Chem.* 88 (2016) 2734-2741.
- [35] K. Chullasat, P. Nurerk, P. Kanatharana, F. Davis, O. Bunkoed, A facile optosensing protocol based on molecularly imprinted polymer coated on CdTe quantum dots for highly sensitive and selective amoxicillin detection, *Sens. Actuators B* 254 (2018) 255-263.
- [36] X. Xu, P. Guo, Z. Luo, Y. Ge, Y. Zhou, R. Chang, W. Du, C. Chang, Q. Fu, Preparation and characterization of surface molecularly imprinted films coated on multiwall carbon nanotubes for recognition and separation of lysozyme with high binding capacity and selectivity, *RSC Adv.* 7 (2017) 18765-18774.

- [37] R. Barabás, G. Katona, E.S. Bogyá, M.V. Diudea, A. Szentes, B. Zsirka, J. Kovács, L. Kékedy-Nagy, M. Czikó, Preparation and characterization of carboxyl functionalized multiwall carbon nanotubes–hydroxyapatite composites, *Ceram. Int.* 41 (2015) 12717-12727.
- [38] P. Nurerk, P. Kanatharana, O. Bunkoed, A selective determination of copper ions in water samples based on the fluorescence quenching of thiol-capped CdTe quantum dots, *Luminescence*, 31 (2016) 515-522.
- [39] J.C. Yorke, P. Froc, Quantitation of nine quinolones in chicken tissues by high-performance liquid chromatography with fluorescence detection, *J Chromatogr A* 882 (2000) 63-77.
- [40] T. Jin, H. Wu, N. Gao, X. Chen, H. Lai, J. Zheng, L. Du, Extraction of quinolones from milk samples using bentonite/magnetite nanoparticles before determination by high-performance liquid chromatography with fluorimetric detection, *J. Sep. Sci.* 39 (2016) 545-551.
- [41] S. Sahoo, C.K. Chakraborti, S.C. Mishra, Qualitative analysis of controlled release ciprofloxacin/carbopol 934 mucoadhesive suspension, *J. Adv. Pharm. Technol. Res.* 2 (2011) 195-204.
- [42] X. Lu, F. Wei, G. Xu, Y. Wu, J. Yang, Q. Hu, Surface molecular imprinting on silica-coated CdTe quantum dots for selective and sensitive fluorescence detection of p-aminophenol in Water, *J. Fluoresc.* 27 (2017) 181-189.
- [43] X. Ren, L. Chen, Preparation of molecularly imprinted polymer coated quantum dots to detect nicosulfuron in water samples, *Anal. Bioanal.Chem.* 407 (2015) 8087-8095.
- [44] M. Li, H. Liu, X. Ren, Ratiometric fluorescence and mesoporous structured imprinting nanoparticles for rapid and sensitive detection 2,4,6-trinitrophenol, *Biosens. Bioelectron.* 89 (2017) 899-905.

- [45] L. Wu, Z.Z. Lin, H.P. Zhong, A.H. Peng, X.M. Chen, Z.Y. Huang, Rapid detection of malachite green in fish based on CdTe quantum dots coated with molecularly imprinted silica, *Food Chem.* 229 (2017) 847-853.
- [46] S. Xu, H. Lu, J. Li, X. Song, A. Wang, L. Chen, S. Han, Dummy molecularly imprinted polymers-capped CdTe quantum dots for the fluorescent sensing of 2,4,6-trinitrotoluene, *ACS Appl. Mater. interfaces* 5 (2013) 8146-8154.
- [47] L. Feng, L. Tan, H. Li, Z. Xu, G. Shen, Y. Tang, Selective fluorescent sensing of  $\alpha$ -amanitin in serum using carbon quantum dots-embedded specificity determinant imprinted polymers, *Biosens. Bioelectron.* 69 (2015) 265-271.
- [48] B. The Huy, M.H. Seo, X. Zhang, Y.I. Lee, Selective optosensing of clenbuterol and melamine using molecularly imprinted polymer-capped CdTe quantum dots, *Biosens. Bioelectron.* 57 (2014) 310-316.
- [49] S.N. Muchohi, N. Thuo, J. Karisa, A. Muturi, G.O. Kokwaro, K. Maitland, Determination of ciprofloxacin in human plasma using high-performance liquid chromatography coupled with fluorescence detection: Application to a population pharmacokinetics study in children with severe malnutrition, *J Chromatogr B* 879 (2011) 146-152.
- [50] B. Prutthiwanasan, C. Phechkrajang, L. Suntornsuk, Fluorescent labelling of ciprofloxacin and norfloxacin and its application for residues analysis in surface water, *Talanta* 159 (2016) 74-79.
- [51] M.K. Pawar, K.C. Tayade, S.K. Sahoo, P.P. Mahulikar, A.S. Kuwar, B.L. Chaudhari, Selective ciprofloxacin antibiotic detection by fluorescent siderophore pyoverdin, *Biosens. Bioelectron.* 81 (2016) 274-279.

- [52] J.M.P.J. Garrido, M. Melle-Franco, K. Strutyński, F. Borges, C.M.A. Brett, E.M.P.J. Garrido,  $\beta$ -Cyclodextrin carbon nanotube-enhanced sensor for ciprofloxacin detection, *J. Environ. Sci. Health A* 52 (2017) 313-319.
- [53] M. Radičová, M. Behúl, M. Marton, M. Vojs, R. Bodor, R. Redhammer, A. Vojs Staňová, Heavily Boron Doped Diamond Electrodes for Ultra Sensitive Determination of Ciprofloxacin in Human Urine, *Electroanalysis* 29 (2017) 1612-1617.
- [54] F.M. Abdel-Haleem, M.S. Rizk, I.H.A. Badr, Potentiometric Determination of Ciprofloxacin in Physiological Fluids Using Carbon Paste and Nano-Composite Carbon Paste Electrodes, *Electroanalysis* 29 (2017) 1172-1179.
- [55] M. Okan, E. Sari, M. Duman, Molecularly imprinted polymer based micromechanical cantilever sensor system for the selective determination of ciprofloxacin, *Biosens. Bioelectron.* 88 (2017) 258-264.

**Table 1.** The determination of ciprofloxacin in chicken muscle and milk ( $n=5$ )

Sample	Added ( $\mu\text{g kg}^{-1}$ )	Found ( $\mu\text{g kg}^{-1}$ )	Recovery (%)	RSD (%)
Chicken muscle I	0.0	0.19	-	-
	1.0	1.16 $\pm$ 0.02	96.2	2.4
	5.0	4.45 $\pm$ 0.21	85.1	4.9
	10.0	9.54 $\pm$ 0.42	93.4	4.5
	50.0	48.35 $\pm$ 1.34	96.3	2.8
Chicken muscle II	0.0	0.19	-	-
	1.0	1.08 $\pm$ 0.02	89.0	3.1
	5.0	4.80 $\pm$ 0.34	92.3	7.4
	10.0	9.69 $\pm$ 0.25	95.0	2.7
	50.0	48.02 $\pm$ 1.31	95.7	2.7
Chicken muscle III	0.0	n.d.	-	-
	1.0	0.95 $\pm$ 0.04	95.4	3.8
	5.0	4.82 $\pm$ 0.13	96.5	2.7
	10.0	9.80 $\pm$ 0.18	98.0	1.9
	50.0	49.03 $\pm$ 0.98	98.1	2.0
Milk I	0.0	n.d.	-	-
	1.0	0.85 $\pm$ 0.05	85.4	5.4
	5.0	4.52 $\pm$ 0.20	90.3	4.4
	10.0	9.44 $\pm$ 0.22	94.4	2.3
	50.0	49.20 $\pm$ 0.46	98.4	0.9
Milk II	0.0	0.35	-	-
	1.0	1.18 $\pm$ 0.01	82.6	1.2
	5.0	4.87 $\pm$ 0.18	90.6	4.0
	10.0	9.88 $\pm$ 0.20	95.2	2.0
	50.0	48.69 $\pm$ 0.64	96.7	1.3
Milk III	0.0	0.22	-	-
	1.0	1.12 $\pm$ 0.03	90.6	2.9
	5.0	4.58 $\pm$ 0.24	87.3	5.4
	10.0	9.58 $\pm$ 0.31	93.6	3.3
	50.0	48.20 $\pm$ 0.83	96.0	1.7

n.d. = not detectable

**Table 2.** Comparison of the developed optosensor with other methods for the determination of ciprofloxacin.

Analytical technique	Samples	Linear range ( $\mu\text{g L}^{-1}$ )	LOD ( $\mu\text{g L}^{-1}$ )	Recovery (%)	RSD (%)	References
HPLC-FLD	Human plasma	20-4,000	10.0	73.0-95.0	3.0-17.0	[49]
HPLC-UV	Human plasma	50-8,000	10.0	90.0-96.0	<4.0	[5]
HPLC-PDA	Sputum samples	50-2,000	17.0	>80.0	<15.0	[4]
HPLC-FLD	Surface water	200-2,000	100	102.5-122.2	9.2	[50]
Electrochemical	Pharmaceutical samples and biological fluids	1.6-281.6	0.56	98.0-103.0	3.0	[9]
Fluorescent siderophorepyoverdine	Pharmaceutical tablet	-	2,362	98.6	1.3	[51]
Electrochemical	Wastewater	3,313-26,507	16.6	98.2-107.0	< 5.0	[52]
Electrochemical	Urine samples	33-3,313	7.3	99.1-109.6	1.0-1.4	[8]
Electrochemical	Urine samples	0.15 - 2.11	0.05	97.0-102.0	2.4	[53]
Electrochemical	Physiological Fluids	3,313-3,310,000	2618	98.7-104.5	0.7-0.9	[54]
MIP based micromechanical cantilever sensor	-	497-50,000	265	94.0	1.4	[55]
COOH@MWCNT-MIP-QDs optosensor	Milk and chicken	0.1-1.0 1.0-100	0.066	82.6-98.4	< 8.0	This work

HPLC = high performance liquid chromatography; FLD = fluorescence detector; UV = Ultraviolet-Visible detector; PAD = photodiode array detector; MIP = molecularly imprinted polymer; QDs = quantum dots; COOH@MWCNT = carboxylic functionalized multiwall carbon nanotubes

## Figure Captions

**Fig. 1** The synthesis of nanocomposite COOH@MWCNT-MIP-QDs optosensors for the specific recognition of ciprofloxacin.

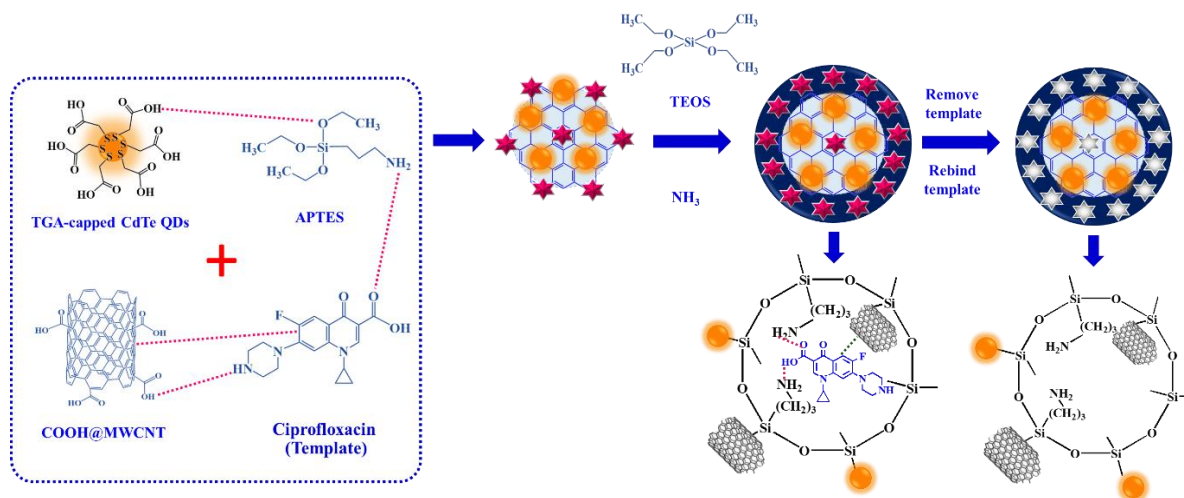


**Fig. 2** Fluorescence spectra of nanocomposite COOH@MWCNT-NIP-QDs (a), COOH@MWCNT-MIP-QDs after removal of template molecule (b) and COOH@MWCNT-MIP-QDs before removal of template molecule (c).

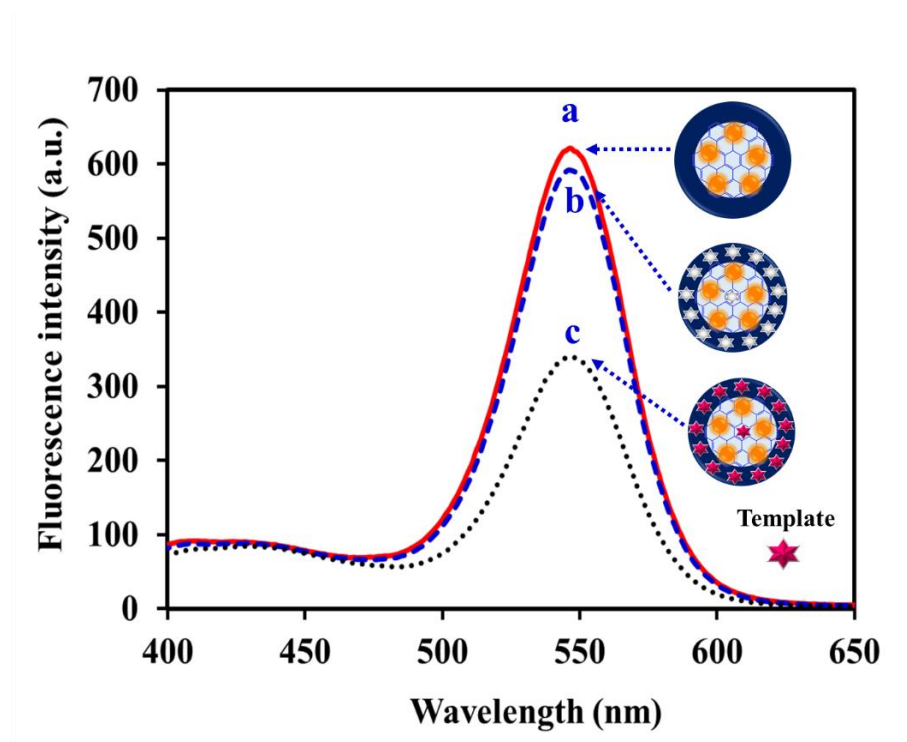


**Fig. 3** TEM images of (A) TGA-capped CdTe QDs, (B) nanocomposite MIP-QDs and (C) SEM image of the nanocomposite COOH@MWCNT-MIP-QDs fluorescence probe.

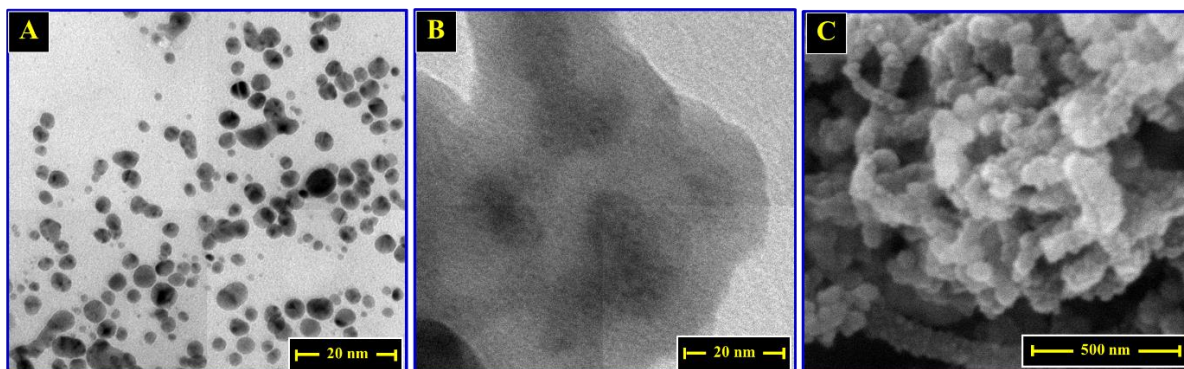


**Fig. 4** FT-IR spectra of (a) TGA-capped CdTe QDs, (b) ciprofloxacin, (c) COOH@MWCNT-MIP-QDs with template molecule (ciprofloxacin), (d) COOH@MWCNT-MIP-QDs without template molecule (ciprofloxacin) and (e) COOH@MWCNT.

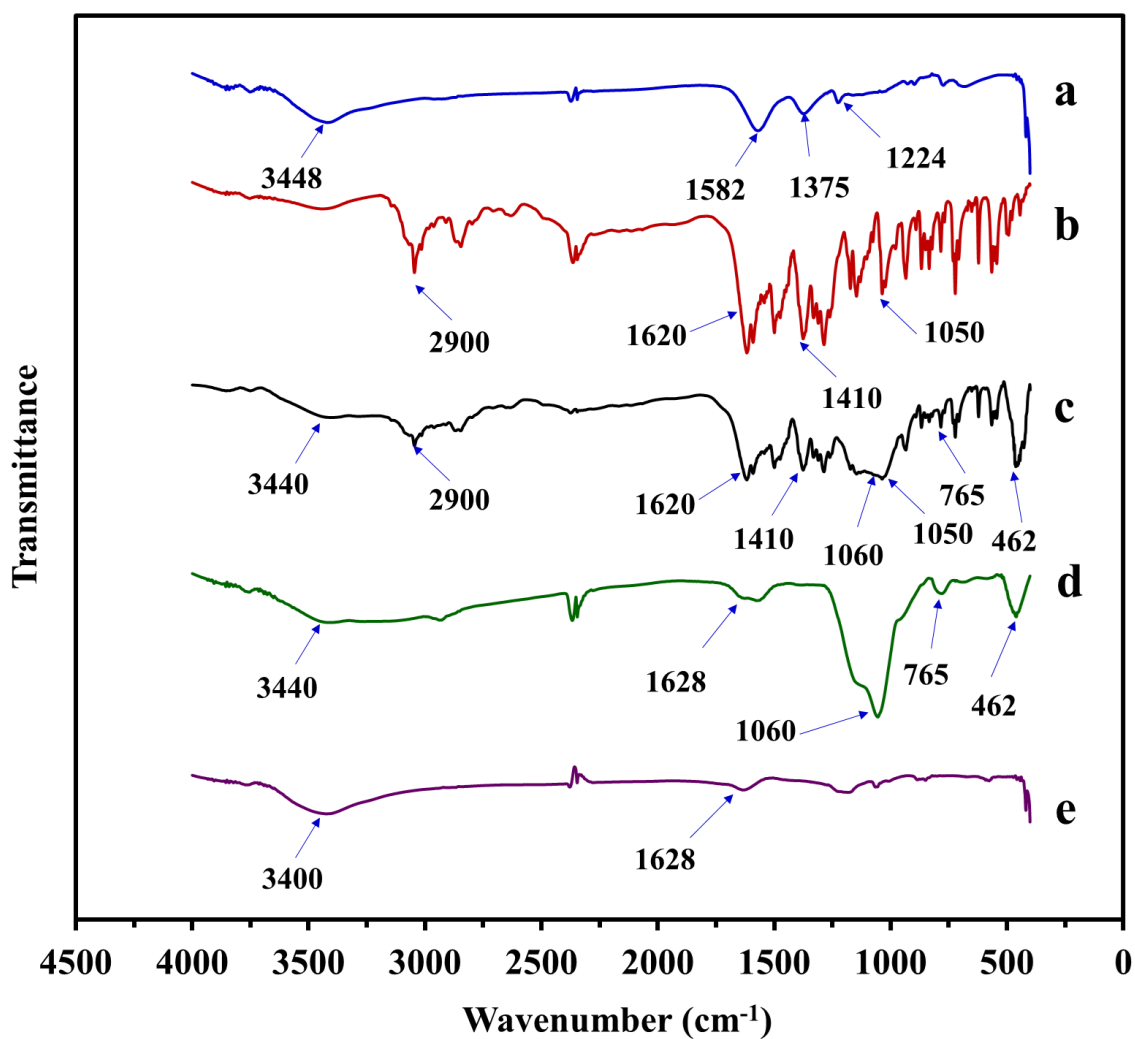


**Fig. 5** (A) Effect of pH, (B) amount of COOH@MWCNTs, (C) molar ratio of template to cross-linker and (D) molar ratio of template to monomer on the fluorescence quenching of nanocomposite COOH@MWCNT-MIP-QDs fluorescence probes for ciprofloxacin detection (n=3)

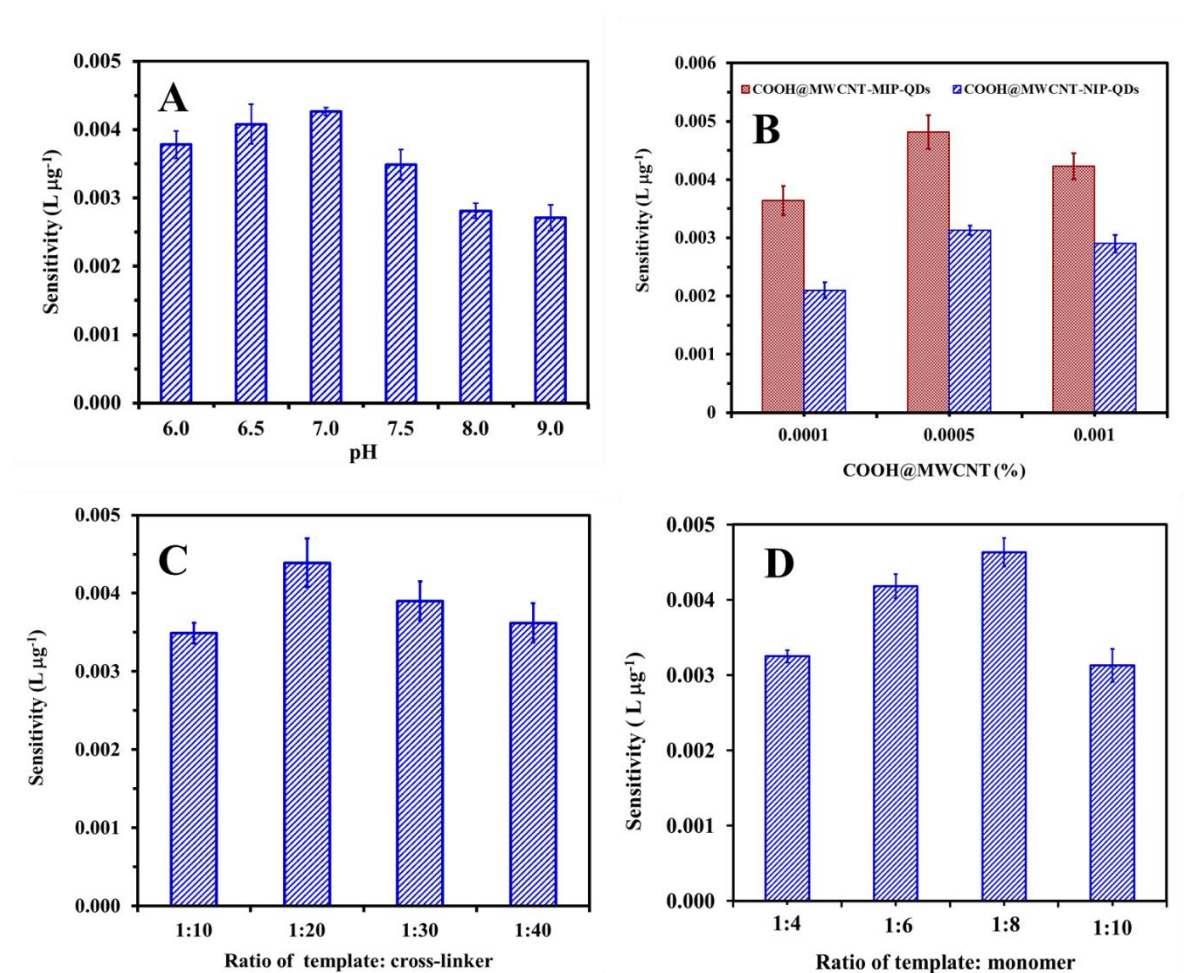


**Fig. 6** The sensitivity of different fluorescence probe for ciprofloxacin detection with an incubation time of 15 min (n=3).

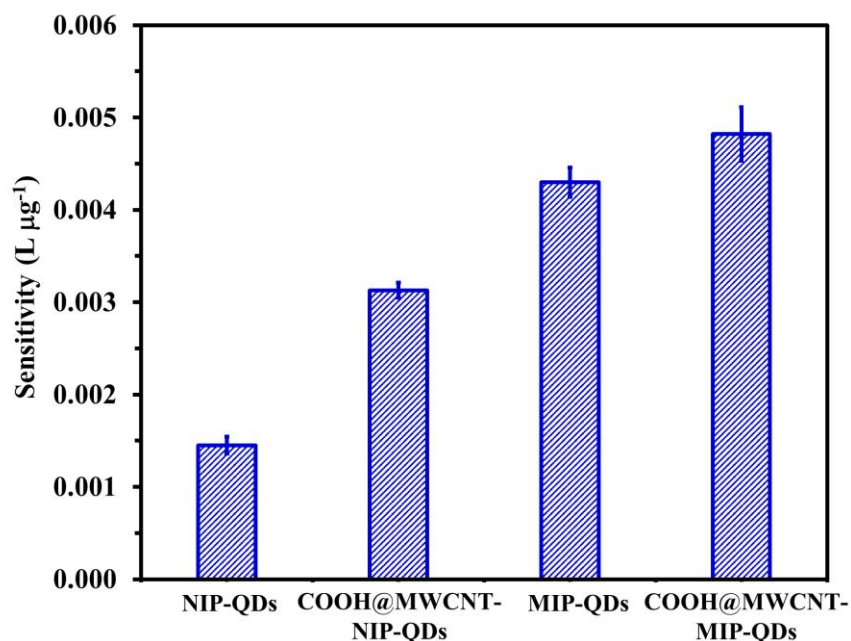


**Fig. 7** The selectivity of nanocomposite COOH@MWCNT-MIP-QDs, COOH@MWCNT-NIP-QDs and NIP-QDs to ciprofloxacin and analogous molecules; (inset) effect of a competitive analog danofloxacin on the binding of ciprofloxacin to the nanocomposite COOH@MWCNT-MIP-QDs. For all results, n=3.

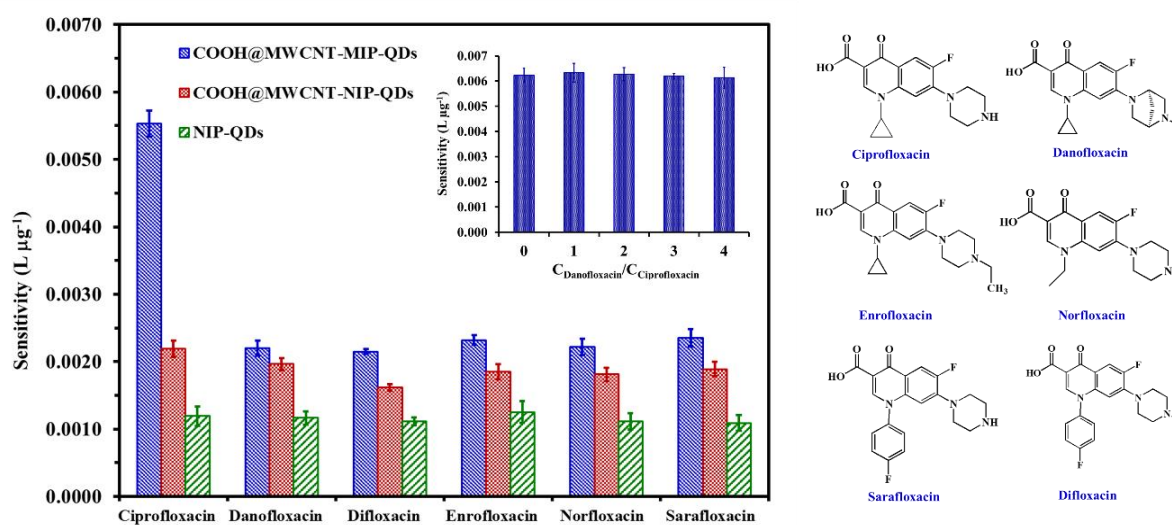


**Fig. 8** (A) The linearity of ciprofloxacin in the concentration range of 0.10-100.0  $\mu\text{g L}^{-1}$ , (B) 0.10-1.0  $\mu\text{g L}^{-1}$ , (C) 1.0-100  $\mu\text{g L}^{-1}$  ( $n=3$ ) and (D) fluorescence spectra of nanocomposite COOH@MWCNT-MIP-QDs with increasing concentration of ciprofloxacin; (inset) photographs of COOH@MWCNT-MIP-QDs in Tris-HCl buffer solution (left) and COOH@MWCNT-MIP-QDs + 1.0  $\text{mg L}^{-1}$  of ciprofloxacin (right) under UV light.

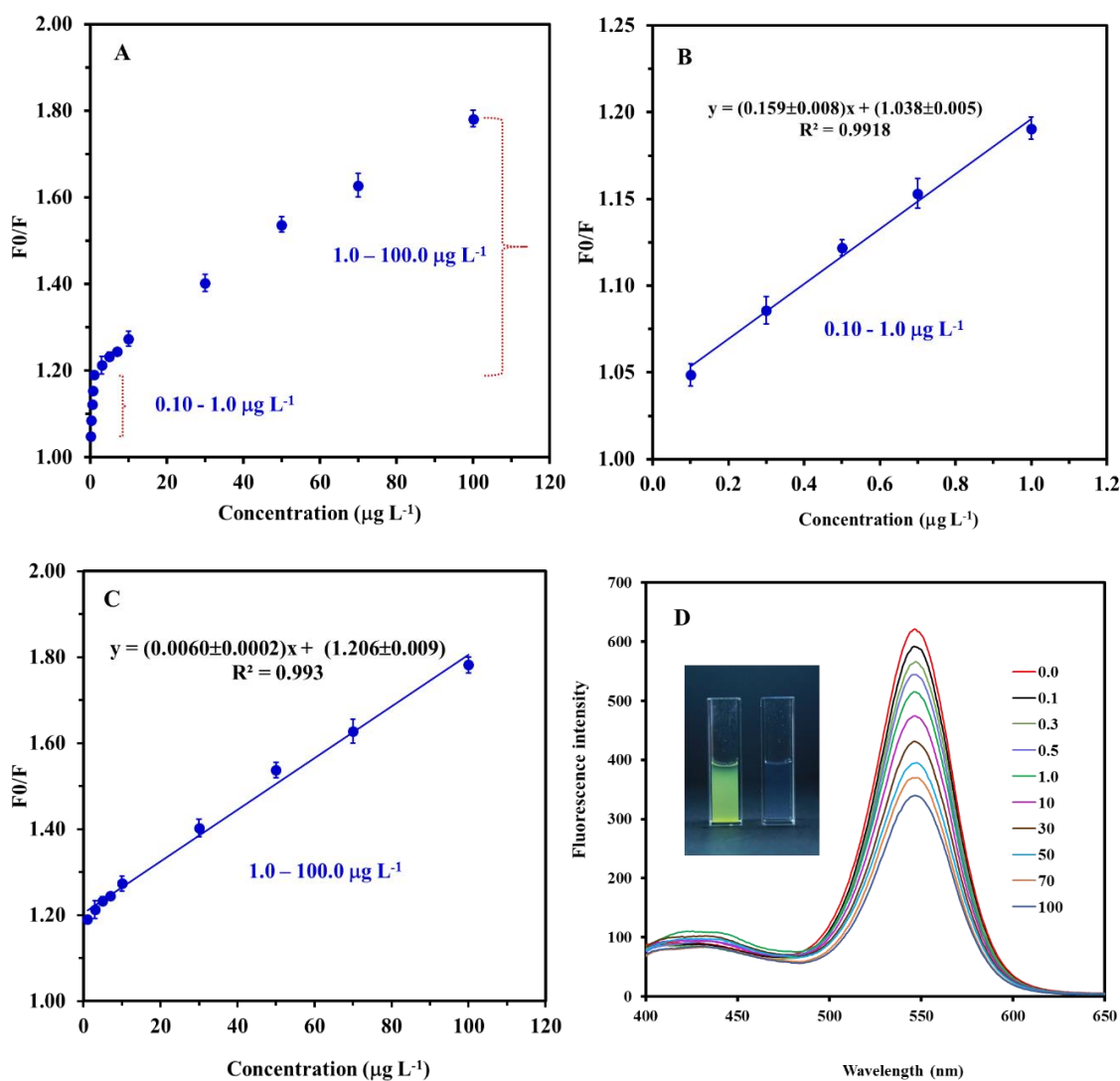


**Fig. 9**(A) HPLC chromatograms of spiked milk samples at different concentration of ciprofloxacin; (a)  $10 \mu\text{g kg}^{-1}$ , (b)  $50 \mu\text{g kg}^{-1}$  (c)  $300 \mu\text{g kg}^{-1}$  and (d)  $500 \mu\text{g kg}^{-1}$ . (B) Correlation between the nanocomposite COOH@MWCNT-MIP-QDs optosensor system and the HPLC method for the determination of ciprofloxacin in milk.

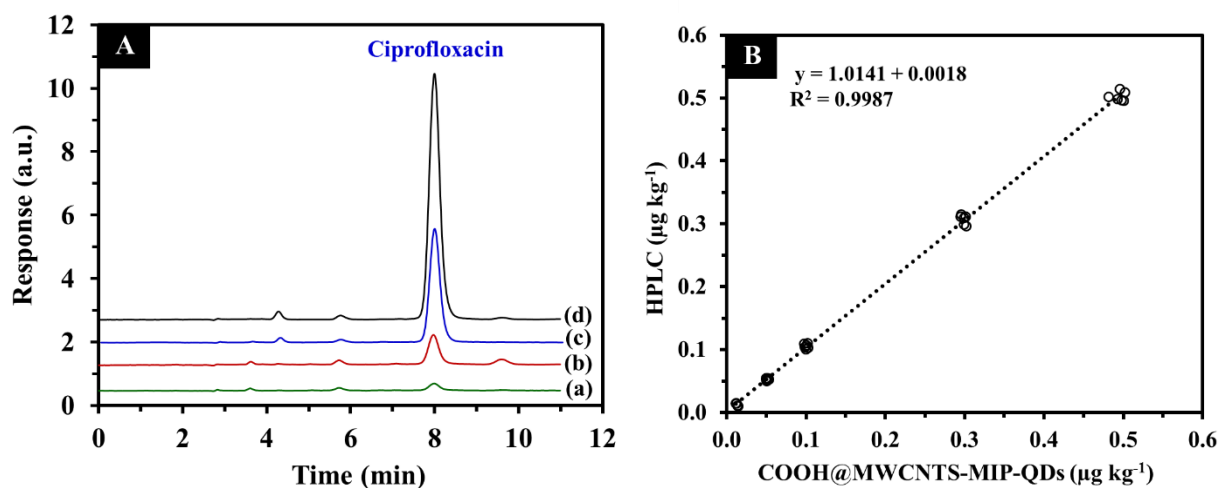


**Fig. S1** UV-Vis spectrum (dot line) and fluorescence emission spectrum (solid line) of TGA-capped CdTe QDs.

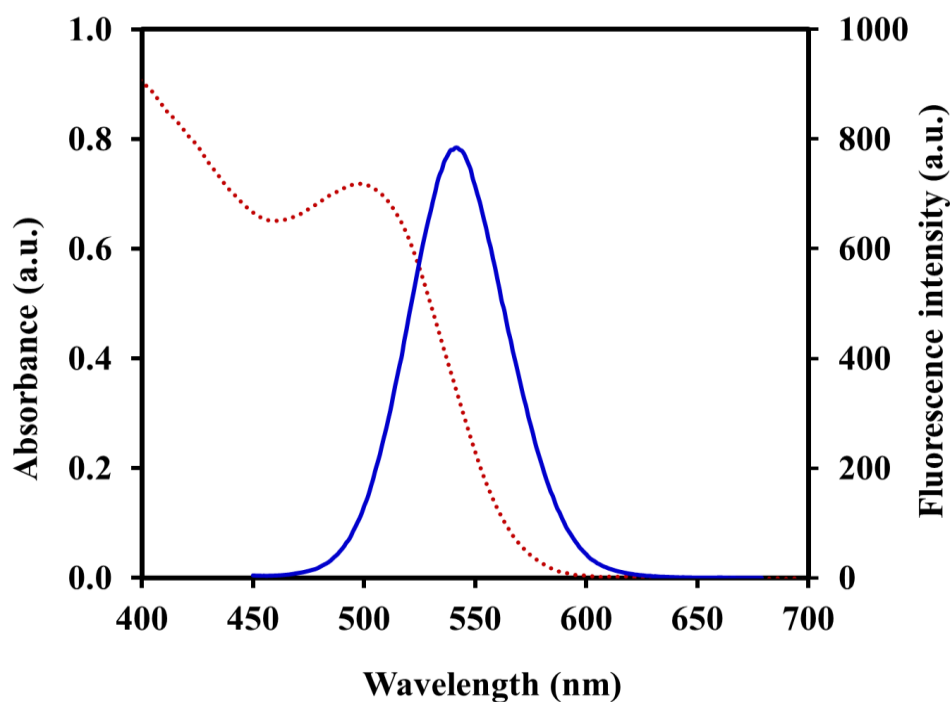


**Fig. S2** Effect of incubation time on the fluorescence quenching of COOH@MWCNT-MIP-QDs and MIP-QDs for the determination of ciprofloxacin ( $n=3$ ).

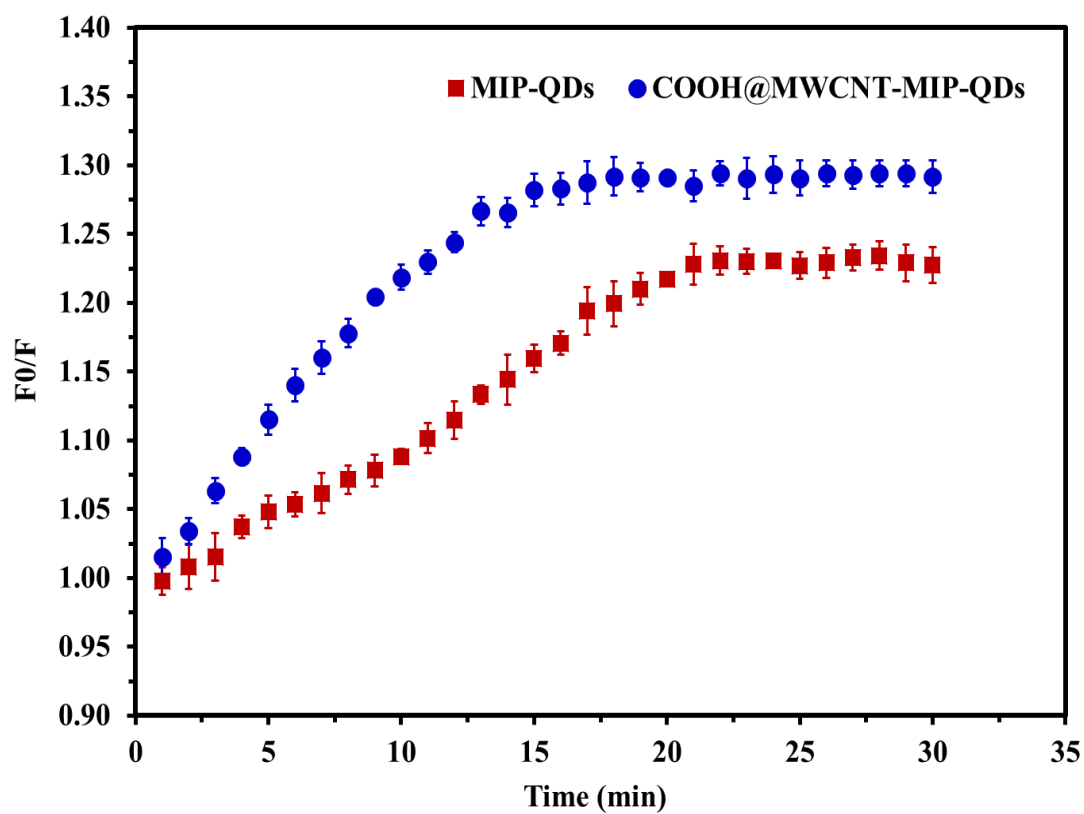


**Fig. S3** Absorption spectrum of ciprofloxacin (a) and emission spectrum of nanocomposite COOH@MWCNT-MIP-QDs (b).

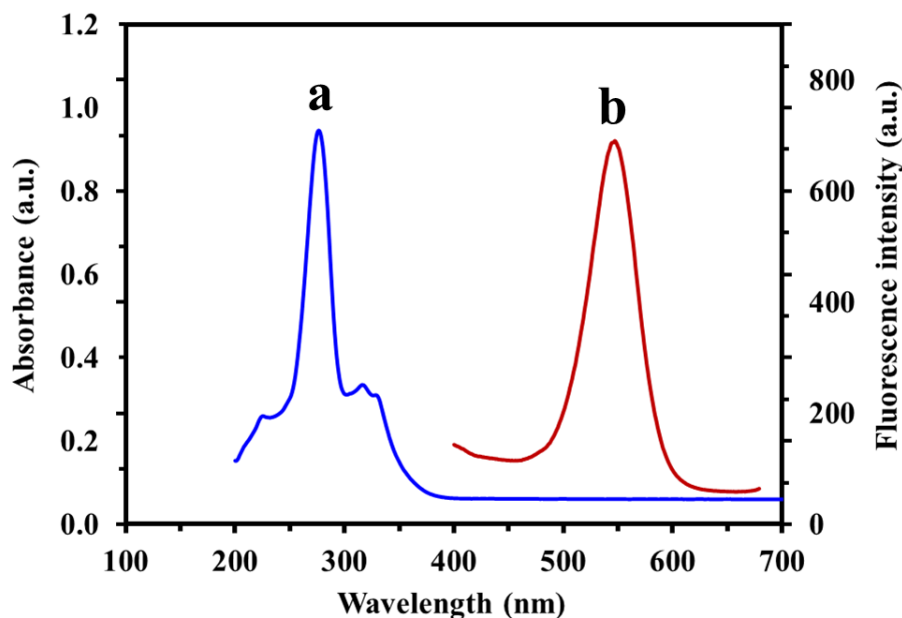


**Fig. S4** The fluorescence stability of nanocomposite COOH@MWCNT-MIP-QDs fluorescence probes and CdTe QDs in 0.01 M Tris-HCl buffer solution (pH 7.0) (n=3)

